8-2019

Modification of Chemical Vapor-Deposited Carbon Electrodes with Electrocatalytic Metal Nanoparticles through a Soft Nitriding Technique

Enoch Amoah
East Tennessee State University

Modification of Chemical Vapor-Deposited Carbon Electrodes with Electrocatalytic Metal Nanoparticles through a Soft Nitriding Technique

---

A thesis

presented to

the faculty of the Department of Chemistry

East Tennessee State University

In partial fulfillment

of the requirements for the degree

Master of Science in Chemistry

---

by

Enoch Amoah

August 2019

Dr. Gregory W. Bishop, Chair

Dr. Dane W. Scott

Dr. Marina Roginskaya

Keywords: Ultramicroelectrodes, nitrided CVD carbon, gold nanoparticles, methanol oxidation

ABSTRACT

Modification of Chemical Vapor-Deposited Carbon Electrodes with Electrocatalytic Metal Nanoparticles through a Soft Nitriding Technique

by

Enoch Amoah

Metal nanoparticles have been widely used for many catalytic and electrocatalytic applications due to their larger surface area-to-volume ratios and higher densities of active sites compared to bulk materials. This has resulted in much interest in understanding the electrocatalytic behavior of metal nanoparticles with respect to their structure. However, most research on this topic has employed collections of nanoparticles. Due to difficulties in controlling and characterizing particle loading and interparticle distance in nanoparticle ensembles, single nanoparticles studies have recently become a topic of great interest. In this study, a soft nitriding technique was applied to chemical vapor-deposited carbon ultramicroelectrodes (UMEs) in order to immobilize ligand-free AuNPs onto the carbon substrate. The feasibility of this method is geared toward studying the properties of single AuNPs immobilized onto carbon nanoelectrodes. The ligand-free AuNPs immobilized onto the nitrided carbon UMEs were highly electrocatalytic toward methanol oxidation.

DEDICATION

This work is dedicated to Mr. Charles Asare, Theresah Agyeiwaa, Kwaku Akowuah, Ellen Asare and Lydia Nsiah.

ACKNOWLEDGMENTS

I am very grateful to God Almighty for how far He has brought me, the great things He has done and the greater things He will do. I can never thank Him enough.

My sincerest gratitude to my advisor Dr. Gregory W. Bishop for his inspirational and academic support supervising this work and through my study period at ETSU. A special thank you to my advisory committee members, Dr. Marina Roginskaya and Dr. Dane W. Scott for their supportive role and helping me build my career as a chemist. I also thank my lab colleagues and friends; George A. Danful, Theophilus Neequaye, Daniel Mawudoku, Chidibere Ogbu, Ebenezer Ametsetor and all those who contributed to the success of this work.

I would also like to acknowledge the American Chemical Society Petroleum Research Fund (Award # 58123 – UN15) for providing funds for this work, ETSU Graduate School for the thesis and dissertation scholarship and ETSU chemistry department for the Margaret Sells endowment scholarship award.

TABLE OF CONTENTS

LIST OF TABLES

Table Page

LIST OF FIGURES

Figure Page

LIST OF ABBREVIATIONS

AuNP – Gold Nanoparticles
CV – Cyclic Voltammetric
CVD – Chemical Vapor Deposition
GNC – Graphitic Nanostructure Carbon
HER – Hydrogen Evolution Reaction
I.D – Internal Diameter
LSV – Linear Sweep Voltammetric
MOR – Methanol Oxidation Reaction
NP – Nanoparticles
O.D – Outer Diameter
ORR – Oxygen Reduction Reaction
PBS – Phosphate Buffer Silane
PtNPs – Platinum Nanoparticles
SCE – Saturated Calomel Electrode
SNP – Single Nanoparticle
UME – Ultramicroelectrode

CHAPTER 1

INTRODUCTION

Metal Nanoparticles and Electrocatalysis

Nanoparticles (NPs), that is particles within the range of 1 to 100 nanometers in size[1–5], have been of significant importance to science and technology for decades. NPs can often exhibit interesting optical properties due to their small size and catalytic behavior towards some reactions as a result of their large surface area-to-volume ratio and higher density of active sites[1,6,7] compared to bulk materials. These benefits of nanoparticles have resulted in many applications in catalysis[8,9], sensors[10–12], conversion of energy and its storage[6], electronics and optics[13–15].

The catalytic and electrocatalytic activities of metal NPs towards various commercially and environmentally important reactions have been extensively explored and utilized. For example, Yan et al. investigated the electrocatalytic behavior of gold nanoparticles (AuNPs) supported on activated carbon towards methanol oxidation reaction (MOR), an important reaction in direct methanol fuel cells, in an alkaline medium[16]. The peak anodic mass activity (current normalized by metal loading in terms of mass)[17] at 0.355 V vs. Hg/HgO increased appreciably to a value of 48.6 mA mg^{-1} as the amount of methanol increases, demonstrating the high electrocatalytic activity of the AuNPs toward methanol oxidation. In another instance, Afraz et al. electrodeposited platinum nanoparticles (PtNPs) of size 85 nm in diameter on graphitic carbon nanostructure (GCN) to study electro-oxidation of methanol in acidic medium[18]. Peak potentials for methanol oxidation were observed at 0.6 V vs. Hg/HgO (forward scan) and 0.45 V (reverse scan) for 0.5 M MeOH in 0.5 M H_2SO_4. However, no methanol oxidation peak was observed for bare GCN substrate in the 0.5 M H_2SO_4 containing 0.5 M MeOH which vividly

shows that the catalytic activity for the methanol electro-oxidation was solely based on the PtNPs.

Effect of Metal Nanoparticles Composition and Size on Electrocatalysis

In addition to particle composition, size and shape have also been found to influence electrocatalytic properties of metal NPs[19]. To understand the effect of nanoparticle size on electrochemical oxidation of methanol, Nart et al. deposited PtNPs of different sizes on carbon supports and studied their electrocatalytic activity toward MOR using differential electrochemical mass spectrometry[20]. These researchers observed that particles of size range between 3 and 10 nm were highly electrocatalytic toward the oxidation of methanol to carbon dioxide. Particles of size outside the 3-10 nm range were less efficient in electro-oxidizing methanol and resulted in partial oxidation of methanol to formaldehyde. The decrease in efficiency of particles <3 nm was attributed to their morphology explained as due to Pt-O binding which occurred at lower coordination sites as well as ensemble effects.

Shao et al[17]. investigated the effect of PtNPs size on electrocatalysis of the oxygen reduction reaction (ORR) in $HClO_4$. By employing the method of copper underpotential deposition on 1.3 nm platinum nanoparticle seeds, Pt nanoparticles of size 1-5 nm diameter were prepared on a Ketjen Black carbon support. According to the study, particles within the range of 1.3 to 2.2 nm showed a significant increase in mass activity towards ORR by a factor of 2-fold, while a decrease in mass activity was observed as the particles size increased beyond 2.2 nm. Also rapid 4-fold increase in specific activity (current normalized by the electrochemically active surface area)[17] was observed for particle growth up to 2.2 nm. However, the increase in specific activity was slowed as the particle size increased. In contrast, a separate study by Gamez et al.[21]

found the catalytic activity of PtNPs towards ORR to decrease with decreasing particle size for particles in the range of 4.3 to 1.2 nm.

Effect of Metal Nanoparticles Spatial Distribution on Electrocatalytic Properties

While electrocatalytic properties of various metal NPs towards many different reactions have been widely studied, understanding the link between physical and electrocatalytic properties remains a key barrier to effective design, optimization, and implementation of NP-based electrocatalysts[22,23]. To date, most of the research focused on metal NP electrocatalysts has involved collections of particles distributed on large conductive surfaces (macroelectrodes)[24]. These studies only provide information about the ensemble average behavior and are subject to effects related to spatial distribution of particles (e.g. interparticle distance, nanoparticle loading, etc.)[25–28], which can often be difficult to predict, control, and characterize.

Higuchi et al. evaluated the effect of nanoparticle loading on ORR using PtNPs dispersed on a carbon black rotating disk electrode in an electrolyte solution of 0.1 M $HClO_4$ saturated with air[28]. Higuchi et al. observed that the area-specific activity for the ORR was not affected by Pt loading in the range of 19.2 to 63.2 wt% Pt-loading levels. In a separate study, Taylor et al. recently reported an inverse relationship between mass activity and NP loading for ORR using PtNPs deposited on a carbon rotating disk electrode[25]. While mass activity decreased with increasing NP loading, specific activity increased with increasing NP loading. This is to say that lower specific activity of the catalyst is expected if the PtNPs are more dispersed. Particles were found to agglomerate upon increasing the loading from 20 to 80 wt%, resulting in a decrease in mass activity of the Pt catalysts.

Kumar and Zuo[27] reported that activity of electrooxidation of carbon monoxide via AuNPs depends on particle size and interparticle distance. They grew uniform arrays of AuNPs

of various sizes (2.4 to 9.0 nm) and interparticle distances (28 to 80 nm) on a rotating disk electrode. Voltammetric results showed that increasing the interparticle distance in arrays of ca. 4 nm AuNPs from 28 to 80 nm resulted in a positive shift of the CO oxidation half-wave potential. This observation was ascribed to the change in diffusion pattern of CO with the interparticle distance. A publication by Nesselberger et al.[29] suggested that the activity of ORR is also affected by interparticle distance. In this study, Nesselberger and co-workers used well-defined, size-selected Pt nanoclusters deposited on glassy carbon substrates. They observed that the activity of closely packed Pt nanoclusters bears resemblance to that of bulk Pt. The activity is affected by surface coverage of oxygenated species, which depends on the distribution of electrochemical potential in the electrochemical double-layer situated between neighboring nanoclusters[25,29].

While advances have been made in documenting relationships between spatial distribution of NPs and electrocatalytic behavior, these aspects of NP ensembles largely remain challenging or costly to control and are often difficult to characterize. Single-nanoparticle electrochemical methods have recently been introduced to evaluate the electrocatalytic properties of individual, isolated NPs in ways that avoid ensemble averaging and spatial distribution effects that can complicate analyses based on collections of particles[6,22,30].

Electrochemical Studies of Single Nanoparticles

Measurements made using individual, isolated NPs present an opportunity to evaluate the important structure-function relationship in the absence of complicating factors related to spatial distribution and heterogeneity[22]. Two main ways of studying single nanoparticles (SNPs) electrochemically are by impact techniques and immobilization. The former involves holding an ultramicroelectrode (UME; an electrode of critical dimension <25 μm) at a constant potential and

measuring the response generated as a single particle collides with the electrode[6,14,26] . In this approach, as a single NP collides with the UME, a small current transient, which can be related to direct NP oxidation or an electrocatalytic reaction depending on the conditions and applied potential, evolves and is measured. Studies of this sort provide information related to particle size, concentration, collision dynamics and transport processes through the magnitude, duration, and frequency of the current-time transient signals[28–35]. Alternatively, a single NP may be immobilized on an electrode so that voltammetry or other electrochemical techniques may be used to evaluate its electrocatalytic properties. Immobilization of a single NP requires a nanometer-sized electrode of comparable or smaller size to the particle to ensure that only a single particle is attached to the nanoelectrode surface[5,23,39]. One of the most challenging aspects of single NPs studies is the fabrication of electrodes required to study these particles of interest.

Fabrication of Electrodes for Single Nanoparticles Studies

UMEs and nanoelectrodes (electrodes with critical dimensions between 1– 100 nm)[40,41,42] offer a handful of advantages applicable in electrochemical studies such as reduced RC time constant and enhanced mass transport as a result of decreased charging current and dominance of efficient radial diffusion[43–45]. UMEs were first developed in the early 1980s by Wightman[43,44] and others.[45,46] Since then, several kinds of UMEs and ultrasmall nanoelectrodes with variety of geometries like ring, sphere, inlaid disk, conical and hemisphere have been fabricated with different materials and methods.

Fabrication of UMEs and nanoelectrodes for single NP studies can be accomplished by insulating a metal wire such as silver, gold, and platinum or a carbon fiber into a pulled glass capillary tube[47–50]. To achieve this, the metal wire or carbon fiber is typically first inserted or aspirated into glass capillary. A laser-assisted pipette puller is used to seal the wire at the center

of the capillary and pull it apart into two pieces with tapered ends. A tiny portion of the insulated metal wire or carbon fiber is then exposed by gentle mechanical polishing or chemical etching. While this method has been used since the 1980s to prepare UMEs, more careful control of pulling parameters and polishing or etching procedures enable production of nanoelectrodes as well[51].

UMEs and nanoelectrodes can also be produced through chemical vapor deposition (CVD) of carbon in thin glass quartz capillary pipettes prepared using a laser-based pipette puller. Fabrication of nanoelectrodes by CVD methods can be easier than laser-based sealing and pulling as post-processing steps like polishing and etching can be avoided in many cases. CVD of carbon in pulled pipettes is done either by using a tube furnace[24,52] or microtorch[53] with methane[51,24] and butane[53] gases used as the carbon source. In both cases, after pyrolytic carbon is deposited into the pipette, electrical contact is made through insertion of conductive wire from the opposite end of the tapered quartz capillary. For example, Actis et al.[53] fabricated nanoelectrodes by using a butane microtorch applied to the outside of a quartz pipette to pyrolyze a butane-propane mixture under argon as it was forced through the pipette. Using this simple method, nanoelectrodes of 30 nm size, which were used in electrochemical analyses of single cells, could be fabricated in less than a minute.

Electrochemical Analysis of Single Nanoparticles by Immobilization Methods

A small number of studies have examined the electrocatalytic activities of single metal nanoparticles by immobilizing them onto nanoelectrode substrates (Table 1). Attachment of a single nanoparticle (SNP) to a nanoelectrode surface has been accomplished through adsorption[5], covalent binding, electrodeposition,[39,54,55] and electrostatic binding[23,24]. Published studies have

mostly focused on gold nanoparticles (AuNPs) and reactions like ORR and the hydrogen evolution reaction (HER).

Table 1: Selected Single Nanoparticle Studies Through Immobilization Technique

Electrode	Nanoparticle	Immobilization Method	Reaction Studied	Reference
10 nm CVD Carbon	10 nm Au	Covalent binding, Electrostatic adsorption, Direct adsorption	HER	52
1-150 nm Carbon fiber	< 50 nm Pt	Electrodeposition	ORR	54
10 nm Platinum	15 nm Au	Amine silane linker	ORR	37
8.9 - 42 nm Platinum	Au	Spontaneous deposition	Reduction of gold oxide	4

Zhang and co-workers[23] employed a Pt nanoelectrode modified with an amine silane linker to study the electrocatalytic activity of a single citrate-capped AuNP towards ORR in alkaline medium. In this publication, 10-30 nm AuNPs were individually immobilized onto separate ~10 nm Pt nanoelectrodes. Immobilization of a single AuNP on the Pt electrode resulted in a shift of -0.07 V for the half-wave potential for ORR confirming electrocatalytic behavior of the single AuNP. Comparison of the half-wave potentials for ORR using 14-24 nm single AuNPs showed that the largest AuNP in the size range exhibited the highest electrocatalytic activity. Despite the very impressive results obtained, one of the major drawbacks was distinguishing between the current from the underlying Pt electrode and the AuNP of interest[24].

In another study, Mirkin et al. investigated the electrocatalytic activity of a single 10 nm AuNP immobilized onto carbon nanoelectrode for the hydrogen evolution reaction (HER) [24]. Three different immobilization strategies (electrostatic adsorption, direct attachment and covalent binding)[24] were employed to attach single AuNPs onto carbon nanoelectrodes that were prepared using CVD in quartz nanopipettes. Direct adsorption of AuNPs onto the carbon

substrate, was achieved by immersing the tip of the carbon nanoelectrode in a solution of AuNPs for 1.5 to 2 hours. Though AuNPs that were immobilized onto the nanoelectrode by direct adsorption exhibited remarkable catalytic activity towards HER, the adsorption process was not well understood, and electrocatalytic activity was lost after a couple of hours. Immobilization of single AuNPs through electrostatic adsorption and covalent binding required modification of the electrode with an electrodeposited polyphenylene film. The polyphenylene film was found to affect the onset potential of the reaction of interest due to its insulating properties. While carbon-based electrodes provide benefits over metal nanoelectrodes as platforms for these types of studies, the development and application of alternative strategies for immobilizing single metal nanoparticles on carbon electrodes should help eliminate complications from the use of a polymer layer and possibly extend these techniques to other electrocatalytic systems.

Immobilization of Bare AuNPs onto Carbon Substrates by "Soft" Nitriding

A recent report by Liu et al.[56] described immobilization of highly electrocatalytically active, ligand-free metal nanoparticles on various carbon supports (i.e. carbon blacks, mesoporous carbons, and activated carbons) through a "soft" nitriding technique. The process involves thermal decomposition of urea (nitrogen source) on carbon, which was found to introduce mostly amine/amide but also pyridinic nitrogen and quaternary nitrogen groups onto the carbon surface. Liu et al. grew highly electrocatalytic ligand-free ultrasmall noble metal nanocatalysts by chemical reduction of metal ion precursors using sodium borohydride on soft-nitrided Printex G carbon black. By comparing cyclic voltammograms of methanol oxidation reaction (MOR), ligand-free metal nanoparticles immobilized onto the carbon support manifested significant electrocatalytic activity towards MOR relative to the capped metal nanoparticles[56].

Electrocatalytic Behavior of Nitrogen-Doped Carbon towards Hydrogen Peroxide Reduction

Not only does nitrogen-doped carbon exhibit enhanced affinity towards metal NP deposition, but it has also been shown to possess electrocatalytic properties specifically towards hydrogen peroxide reduction. For example, Shi et al.[57] showed that nitrogen-doped graphene nanoribbons demonstrated improved electrocatalytic behavior towards hydrogen peroxide reduction reaction (Eqns. 1-3) and attributed the main nitrogen groups responsible for this to pyridinic and pyrrolic nitrogen. It is reported that nitrogen atoms provide active sites for electrocatalysis by introducing free electrons into the carbon structure, which promotes O-O bond breakage in H_2O_2 (Eqn. 1).[57]

$$H_2O_2 + e^- \longrightarrow OH_{ad} + OH^- \quad (1)$$

$$OH_{ad} + e^- \longrightarrow OH^- \quad (2)$$

$$2OH^- + 2H_+ \longrightarrow 2H_2O \quad (3)$$

Research Objectives

In this study, soft nitriding of carbon UMEs was explored as a method for immobilizing electrocatalytically active bare gold nanoparticles on small carbon electrodes. Carbon UMEs were prepared based on a simple, fast, low-cost previously reported CVD technique[53] and nitrogen-doping and immobilization of gold nanoparticles were accomplished using methods inspired by previous reports[57,58]. Electrochemical techniques were used to characterize modified CVD carbon electrodes and immobilized AuNPs. Since a previous report[56] showed that AuNPs deposited onto soft-nitrided carbon supports are electrocatalytic towards MOR, electrocatalytic behavior of AuNPs on nitrogen-doped CVD carbon electrodes towards MOR was similarly studied here. The viability of this method for immobilizing highly active AuNPs on carbon

UMEs is investigated in order to determine its potential as a platform for studying the electrocatalytic properties of single, isolated metal nanoparticles using carbon nanoelectrodes.

CHAPTER 2

EXPERIMENTAL

Materials

All chemicals employed in these studies were used as received from the manufacturer. Potassium chloride, 30% (w/w) ammonium hydroxide and ferrocene methanol were obtained from Sigma-Aldrich. Tetrachloroaurate (III) trihydrate was purchased from Alfa Aesar. Hydrogen peroxide, sodium borohydride, sodium phosphate dibasic, sodium chloride and potassium phosphate monobasic were all obtained from Fisher Scientific. Sodium hydroxide beads and hydrochloric acid were purchased from BDH chemicals. Propane/butane mixture was purchased from The Coleman company Inc. Quartz glass capillaries were supplied by Sutter Instrument Company. All aqueous solutions used in these studies were prepared with 18.2 MΩ·cm ultrapure water, made by passing deionized water through a Millipore Synergy purifier. Phosphate-buffered saline (PBS) solution was prepared by dissolving 1.44 g Na_2HPO_4, 8 g NaCl, 0.2 g KCl, and 0.24 g KH_2PO_4 to 0.8 L of ultrapure water. The pH was adjusted to 7.4 using HCl and NaOH. The solution was diluted to 1 L by adding ultrapure water.

Fabrication of CVD Carbon Electrodes

Quartz capillaries (1.0 mm O.D, 0.5 mm I.D) were pulled using a Sutter Instruments P-2000 laser-based micropipette puller. Parameters applied to the pipette puller were: Heat 850, Filament 4, Velocity 36, Delay 140, Pull 50. It should, however, be noted that these parameters are dimensionless and hence not a true depiction of velocity and temperature[51]. Using a propane/butane (30:70) mixture as the carbon source and argon as the protecting gas, a layer of carbon was deposited inside the quartz pipette (Figure 1) by a previously reported microtorch chemical vapor deposition method[53], resulting in CVD carbon ultramicroelectrodes (UMEs). To

make an electrical connection to the CVD carbon, a stainless-steel wire was inserted into the quartz capillary through the unfilled end.

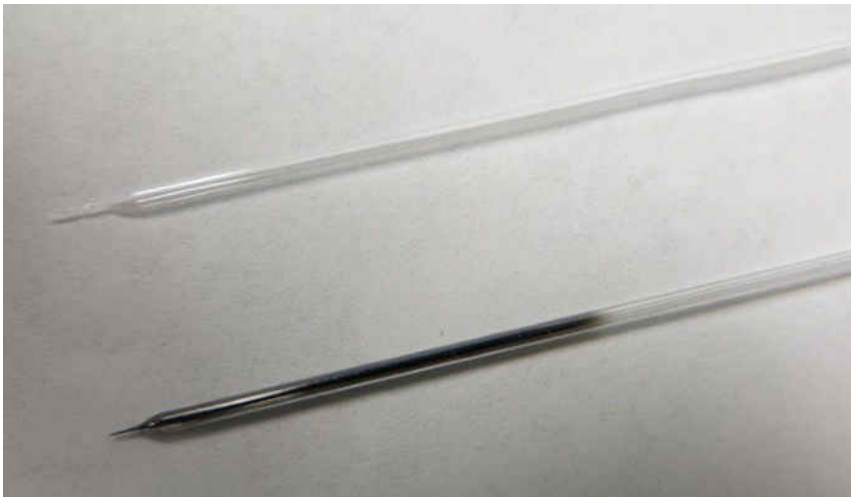

Figure 1: Images of pulled quartz pipette (1.0 mm O.D., 0.5 mm I.D., 10 cm length) before (top) and after (bottom) deposition of carbon.

Nitrogen Doping of CVD Carbon UMEs

Nitrogen-doping was achieved using ammonium hydroxide to modify the CVD carbon electrodes. Briefly, CVD carbon UMEs were suspended in an aqueous solution of ammonium hydroxide (2% w/w) and heated to 80 °C[57]. Electrodes were then rinsed with deionized water and acetone to remove any unreacted species and allowed to dry for studies.

Immobilization of Gold Nanoparticles

AuNPs were immobilized on UMEs via $NaBH_4$ reduction of $HAuCl_4$ through slight modification of previously reported method[58]. Succinctly, a nitrided- or untreated- CVD carbon UME was suspended in a 10 mL of 1 mM $HAuCl_4$ solution for 1 minute, and 30 µL of freshly prepared ice-cold 0.1 mM $NaBH_4$ was quickly added immediately while stirring for 5 to 30

minutes. The solution immediately changed to pink upon addition of $NaBH_4$ which signifies that NPs are formed.

Electrochemical Characterization of Electrodes

All electrochemical measurements in these studies were obtained at room temperature using a Bioanalytical Systems Epsilon electrochemical workstation in potentiostatic mode. A two-electrode system was used for the cyclic voltammetry and linear sweep voltammetry (LSV) measurements with the CVD carbon electrode serving as the working electrode and an Ag/AgCl containing 3 M NaCl fill solution as the reference/counter electrode. CV experiments for immobilized AuNPs characterization were taken in a 0.1 M $HClO_4$ by sweeping the working electrode potential from -0.2 to 1.4 to -0.2 V at a rate of 0.1 V/s. In LSV experiments, the electrodes were placed in 0.01 M KBr and 0.1 M $HClO_4$ solution, and the working electrode potential was scanned from 0.0 to 1.2 V at a rate of 0.001 V/s.

For electrode characterization, the cyclic voltammetric (CV) response was taken in a solution of 0.1 M potassium chloride containing 0.5 mM ferrocenemethanol (redox probe). Working electrodes in the micrometer size range demonstrated sigmoidal CV responses for faradaic reactions in ferrocenemethanol solution[59]. The size (radius) of the disk-shaped ultramicroelectrode was estimated using the steady-state limiting current via the equation:[35,60,61]

$$i_{ss} = 4nFDCr \qquad (4)$$

Where i_{ss} is the steady-state limiting current, n is the number of electrons associated with the redox reaction per molecule, F is Faraday's constant (96484.56 C/mol at 25 °C), D and C are the diffusion coefficient (cm^2/s) and bulk concentration (mol/cm^3) of the redox probe, respectively.

The diffusion coefficient of the redox probe (ferrocenemethanol) used in these studies is 7.80×10^{-6} cm^2 s^{-1}.[7,52,59,62]

Electro-Oxidation of Methanol

A two-electrode system was used with a saturated calomel electrode (SCE) and CVD carbon ultramicroelectrode as the reference and working electrodes, respectively. Prior to each measurement, high-purity nitrogen was bubbled through the solution for 15 minutes. Voltammetric measurements were taken in a 0.1 M NaOH (5 ml) solution and in the same solution in the presence of methanol at various concentrations (104 and 209 uL of 25 M methanol, respectively) using sweep potential -0.5 to +0.6 to -0.5 V vs SCE at a scan rate of 50 mV/s.

Electrochemical Reduction of Hydrogen Peroxide

In electrochemical reduction of hydrogen peroxide, a two-electrode system was used with CVD carbon ultramicroelectrode as the working electrode and silver-silver chloride (Ag/AgCl) electrode as reference electrode. Voltammetric experiments were carried out in 10 ml of 0.05 M PBS (pH 7.4) solution in the absence and presence of 10 mM hydrogen peroxide (10 uL of 10 M hydrogen peroxide). The working electrode potential was scanned from -0.6 to 0.8 to -0.6 V at a rate of 50 mV/s.

CHAPTER 3

RESULTS AND DISCUSSION

Voltammetric Response of Electrodes

CVD carbon electrodes exhibited typical sigmoidal-shaped cyclic voltammetric behavior towards the oxidation of common redox probe ferrocenemethanol (Figure 2). Limiting currents from CV measurements with ferrocenemethanol were used to determine electrode sizes based on equation 1. The average effective radius for CVD carbon electrodes prepared for these studies was 3.1 (± 0.6) µm (n = 7).

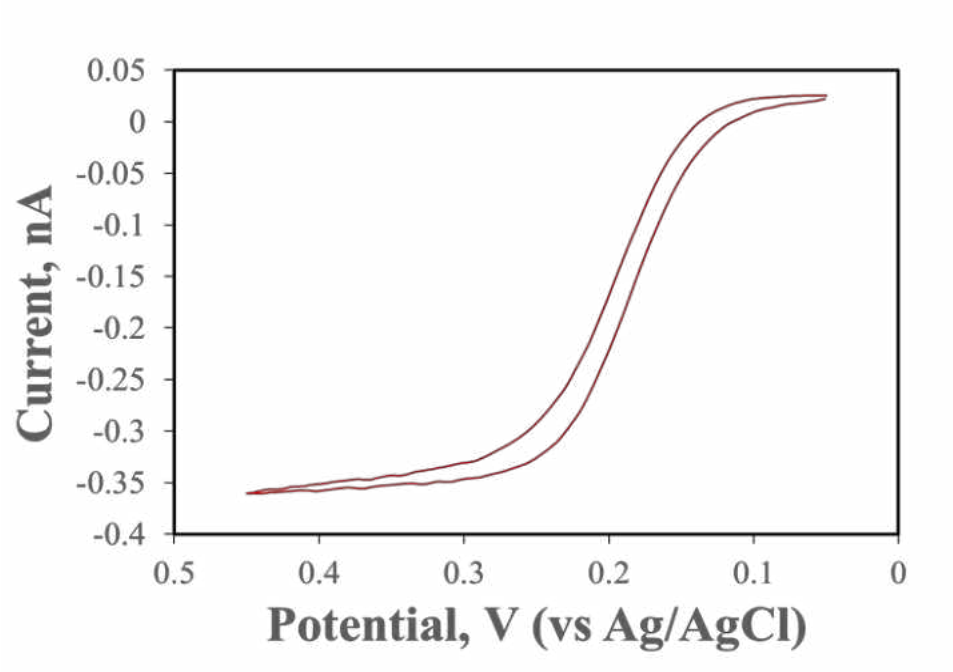

Figure 2: Representative cyclic voltammogram of a CVD Carbon-UME in 0.5 mM ferrocenemethanol with 0.1 M KCl at a scan rate of 10 mV/s

Electrocatalytic Behavior of Nitrided CVD Carbon Electrodes Toward Hydrogen Peroxide

Previous reports[57] indicated that nitrogen-doped carbon materials can exhibit electrocatalytic behavior towards hydrogen peroxide reduction. Therefore, CV responses of

unmodified and nitrogen-doped CVD carbon electrodes were compared in the presence and absence of hydrogen peroxide in order to investigate the viability of the nitrogen-doping process (Figure 3). The nitrogen-doped electrode showed good electrocatalytic behavior toward H_2O_2 reduction as indicated by a significant increase in reduction current (Figure 3B) compared to the unmodified electrode (Figure 3A) and a positive shift in onset potential to -0.095 V in the presence of H_2O_2. In comparison, the onset of H_2O_2 reduction occurred at -0.199 V using the bare electrode. [57] These results seem to be consistent with those of other examples of nitrogen-doped carbon electrodes previously reported in literature. For example, Shi et al.[57] found the onset potential for the H_2O_2 reduction reaction to be -0.15 V using a glassy carbon electrode modified with nitrogen-doped graphene nanoribbons, while the onset potential for the same reaction on the unmodified electrode was -0.3 V vs. Ag/AgCl.

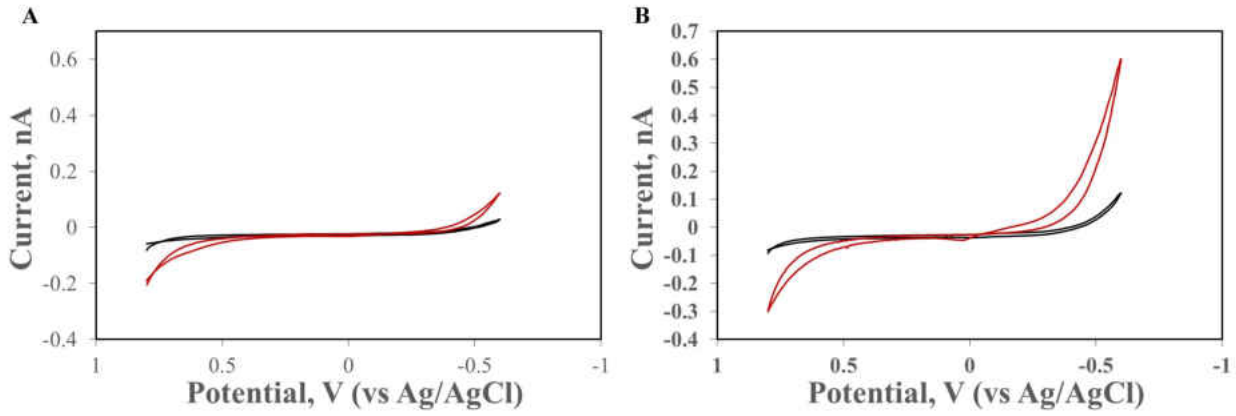

Figure 3: Responses of untreated (A) and nitrogen-doped (B) CVD carbon UMEs in the absence (black) and presence (red) of 10 mM H_2O_2 in PBS (pH 7.4) at a scan rate 50 mV/s.

Immobilization of Au Nanoparticles onto Untreated and Nitrogen-doped CVD Carbon Electrodes

According to recent reports, nitrogen-doping of mesoporous carbons and carbon blacks enables immobilization of highly electrocatalytic, ligand-free nanoparticles onto these carbon surfaces[57,63]. Recent studies from our research group has shown that nitriding carbon fiber can increase the amount of nitrogen signifcantly[64] and enable deposition of gold onto the electrode surface. In the present work, a comparative study was carried out on untreated and nitrided CVD carbon electrodes to determine the effectiveness of depositing ligand-free (bare) AuNPs on these platforms.

Using sodium borohydride as a reducing agent, direct chemical reduction was employed to reduce $HAuCl_4 \cdot 3H_2O$ onto both unmodified and nitrided CVD carbon electrode substrates. After attempting deposition for a duration of 30 minutes on each, CV experiments (Figure 4) were carried out to probe for possible presence of gold on the electrode surfaces through characteristic peaks associated with the oxidation of Au, which typically occurs between +1.2 and +1.4 V vs. Ag/AgCl, and reduction of Au oxide, which is usually observed around +0.60 to +0.85 V vs. Ag/AgCl[60]. Immobilization of Au on nitrided electrodes appeared to be successful as evidenced by the appearance of a broad peak at +1.16 V in the anodic scan and another at +0.824 V in the cathodic scan after deposition was carried out for 30 minutes (Figure 4B). In contrast, untreated electrodes showed no peaks in these ranges (Figure 4A).

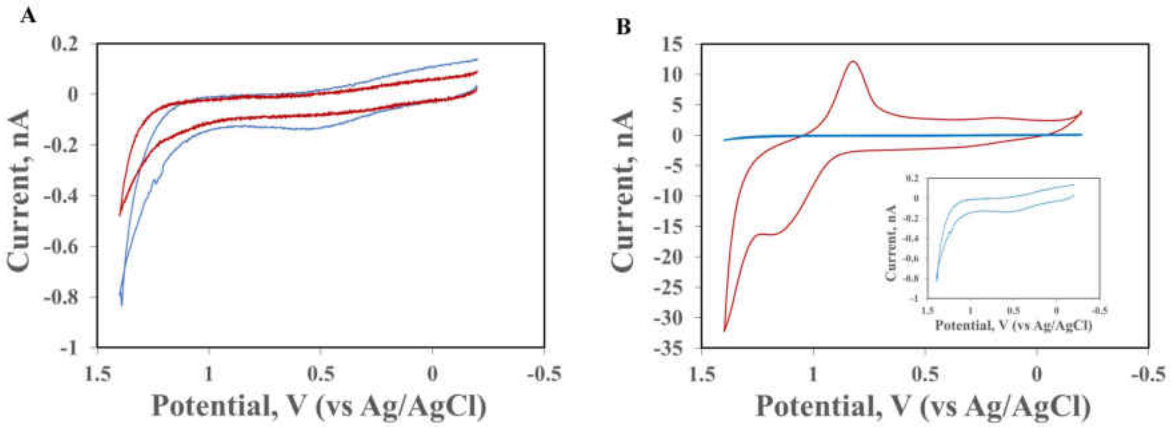

Figure 4: Responses of untreated (A) and nitrogen-doped (B) CVD carbon UME in 0.1 M $HClO_4$ before (blue) and after 30 minutes of (red) attempted immobilization of AuNPs.

By integrating the oxide-reduction peak, the associated charge can be used to estimate the coverage of the AuNPs[65]. The charge associated with the formation or reduction of a monolayer of gold oxide is 400 μC/cm^2.[60,65] The integration of the oxide-reduction peak gave a charge of 9.75×10^{-9} C, and the associated electroactive surface area of 2440 μm^2.

Characterization of AuNPs Immobilized on CVD Electrodes

AuNPs immobilized onto the nitrogen-doped CVD carbon electrodes were characterized using recently reported electrochemical methods[66,67]. Assuming that the AuNPs are spherical in shape, the size can be estimated using surface-area-to-volume ratio, which can be determined from electrochemical signals associated with surface oxide formation and complete oxidative dissolution of AuNPs in the presence of bromide. The charge (in coulombs, C) associated with the formation of Au oxide in $HClO_4$ (Figure 4B) is proportional to the surface area (SA), while the charge (in C) associated with the total oxidative dissolution of the spherical AuNPs in the presence of KBr to form aqueous soluble $AuBr_4^-$ (Figure 5) is proportional to the volume (V).

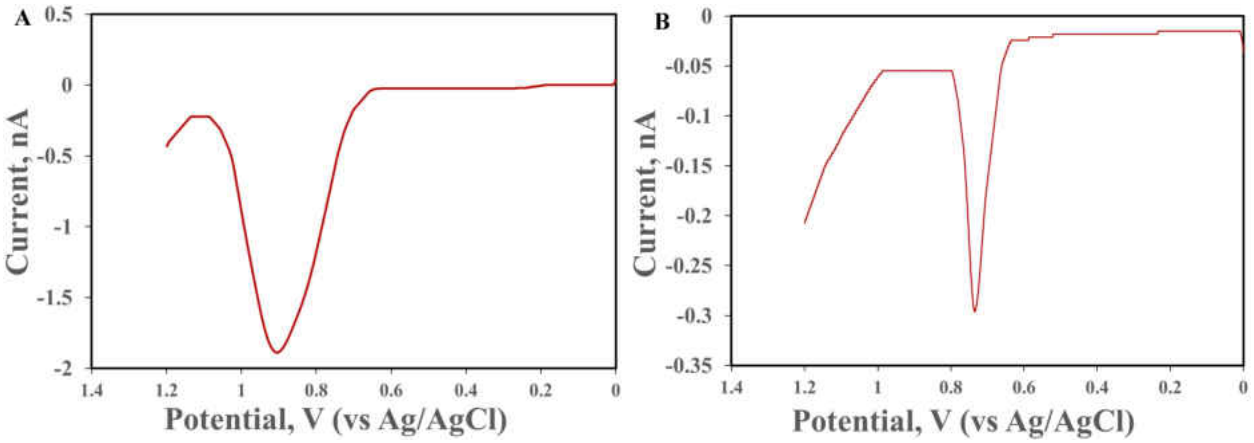

Figure 5: Representative LSVs of nitrided CVD carbon UME in 0.1 M $KClO_4$ with 0.01 M KBr_4 after 5 minutes of attempted Au immobilization pH 4.6(A) and pH 2.5(B) at scan rate 1 mV/s. The peaks at 0.902 and 0.738 V corresponds to oxidative dissolution of Au to $AuBr_4^-$.

Since the surface area and volume of a sphere of radius r are $4\pi r^2$ and $4/3\pi r^3$, respectively, the radius of the Au nanospheres can be estimated through the use of equation 2.[66]

$$\frac{SA}{V} = \frac{3}{r} \qquad (5)$$

where SA and V correspond to the charges (in C) related to the surface area and volume, respectively, of the AuNPs as obtained by integrating the peaks associated with these processes from CV and linear sweep voltammetric (LSV) experiments. This method enables fast and easy determination of particle size and has shown good agreement with sizes determined by transmission electron microscopy for AuNPs ranging from 15 to 70 nm in diameter[66].

Electrochemical surface area-to-volume ratios were used to estimate the sizes of AuNPs immobilized onto nitrided CVD carbon UMEs with varying deposition time and pH (Table 2). Our results indicate that mostly large particles were deposited on the electrodes. For comparison, Liu and coworkers[56] obtained remarkably smaller sized ligand-free Au nanoclusters (average size <2 nm) on nitrogen-doped commercially obtained Printex G carbon when the pH range was 4–10. However, relatively larger particles in the range of 6–10 nm were obtained when the pH was outside the 4–10 range. We obtained larger-sized particles compared to Liu and coworkers

probably because their studies were done on carbon powders of large surface area which contain many active sites for particle nucleation. In our case, the electrode sizes were comparatively small and therefore larger particles and/or aggregation of small particles probably occurred as there are presumably much fewer nucleation sites overall, which would have resulted in less competition for particle growth during the reduction of $HAuCl_4$.

Table 2: Characterization of AuNPs Based on SA/V Ratio Measurements

Time/min	pH	CV Surface Area (nC)	LSV Volume (nC)	Surface Coverage (C/cm^2)	Radius from SA/V (nm)	LSV Peak Position (mV)
5	4.6	13.3776	205.8213	3.0×10^{-1}	46	907
15		07.6173	19.1806	2.5×10^{-2}	9	910
30		21.7144	559.4034	2.5×10^{0}	69	908
5	2.5	00.2414	11.0796	3.4×10^{-3}	138	738
15		02.0514	140.5838	5.1×10^{-1}	206	972
30		01.0771	176.8399	8.3×10^{-2}	60	1075

While the electrochemical surface area-to-volume ratio has shown good agreement with electron microscopy measurements and enables estimation of particle size without necessary knowledge of surface coverage (i.e. the number of particles on the electrode), there are limits to the application of this method[66]. The charges used to calculate the surface area-to-volume ratio are proportional to the surface coverage, and it was reported that whenever the charges are large (meaning surface coverage is high), SA/V ratios are lower than expected. This is because larger surface coverages lead to aggregation of particles as particles come into contact with one another, thereby leading to a decrease in surface area. In previous studies[66], best results in using the electrochemical SA/V ratio method for particle sizing were obtained when the coverage of

the particles was of the magnitude of 10^{-5} C or less for particles of 15 nm radius, though smaller-sized particles exhibited little-to-no significant change in SA/V ratio for coverages as large as 10^{-4} C in magnitude.

In our studies, surface coverages were in the 10^{-9} C range. However, it should be noted that Sharma et al. obtained SA/V ratio measurements using larger indium tin oxide-coated electrodes (1.4 cm^2)[67], so it seems that charge density would be more appropriate than absolute charge in terms of defining surface coverage (Table 2). Based on the areas of our electrodes, the magnitude of the charge density related to surface coverage was in the range of 10^{-3} to10^{0} C/cm^2, which is much larger than the charge densities associated with the studies of Sharma et al. (10^{-6} to 10^{-4} C/cm^2)[67]. Therefore, electrochemical SA/V ratio for particles in our studies shows that the AuNPs were mainly large particles.

It has been reported theoretically and experimentally by Plieth[68] and Henglein[69] that the peak potential associated with oxidative dissolution of metal nanoparticles increases with increasing particle size. Ivanova and Zamborini found that experimental average peak potentials for the oxidative dissolution of 4 to 61 nm diameter AuNPs ranged from +734 to 910 mV vs. Ag/AgCl[67]. However, particles of increasing size exhibited decreasing differences in peak potentials such that 249 nm particles exhibited an average oxidative dissolution peak of 913 mV, compared to 910 mV for 61 nm particles. Our results for AuNPs deposited at pH 4.6, indicate that large particles and aggregates were produced in a way that did not depend on time as oxidative dissolution peaks were all around 910 mV. This result for particles obtained after 15 minutes of deposition at pH 4.6 is inconsistent with sizing by electrochemical SA/V, which could indicate that some particles may have delaminated from the electrode surface or were somehow otherwise removed between the surface area and volume voltammetric measurements, which

would have led to a lower than expected charge for the oxidative dissolution and an overestimation of SA/V. Interestingly, the oxidative dissolution peak positions for particles deposited at pH 2.5 showed a wide distribution, ranging from +738 to 1075 mV. While the peaks at more positive potentials are consistent with large aggregates implied from electrochemical SA/V measurements, the occurrence of the oxidative dissolution peak at +738 mV for the particles obtained after 5 minutes of deposition is intriguing as it suggests very small particles. However, this contradicts electrochemical SA/V measurements. An underestimate of charge associated with surface area due to surface contamination or the high surface coverage may have suppressed the SA/V ratio in this case. This is suspected because the presence of surface contaminants or ligands on the surface of the AuNPs aggregation due to high surface coverage are both known to lead to incomplete oxidation of the Au surface atoms[66].

Electrocatalytic Activity of AuNPs Immobilized on CVD Carbon UMEs

Though electrochemical characterization indicated that deposition mostly resulted in large AuNP aggregates on the CVD carbon UME surface, the electrocatalytic behavior of the bare gold nanoparticles immobilized onto the nitrided CVD carbon UMEs towards methanol oxidation was investigated. To understand the electrocatalytic performance of AuNPs immobilized onto nitrided CVD carbon electrode, comparative experiments were first carried out using bare and nitrided CVD carbon UMEs without immobilized AuNPs. Neither untreated nor nitrided CVD carbon UMEs exhibited significant electrocatalytic activity towards methanol oxidation in deoxygenated 0.1 M NaOH (Figure 6).

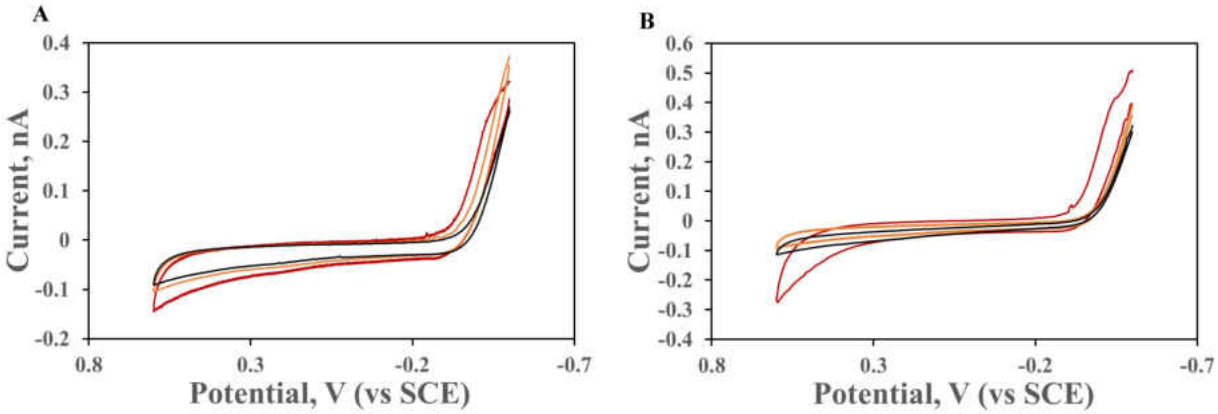

Figure 6: Representative cyclic voltammograms of untreated (A) and nitrogen-doped (B) CVD carbon UME in 0.1 M NaOH in the absence (black) and presence of 0.5 M (orange) and 1 M (red) methanol at a scan rate 50 mV/s.

The CV response of the Au-deposited nitrided CVD carbon was also investigated in deoxygenated 0.1 M NaOH with and without methanol (Figure 7). The Au modified electrode showed clear electrocatalytic behavior toward methanol oxidation as indicated by the increase in oxidation peak current at +0.361 V vs. SCE upon addition of methanol. [16]

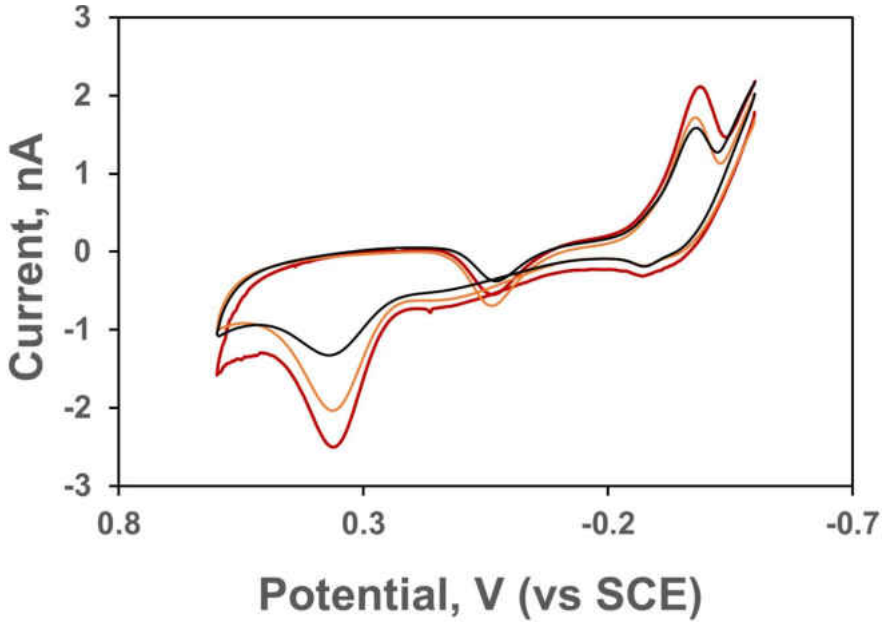

Figure 7: Response of AuNP-modified UMEs in 0.1 M NaOH in the absence (black), presence of 0.5 M (orange) and 1 M (red) methanol at scan rate 50mV/s.

The anodic peak potential of the forward scan observed at 0.361 V vs. SCE (1.383 V vs. the reversible hydrogen electrode, RHE) results from concurrent Au oxide formation and methanol oxidation and is comparable to what has been reported in literature[58,16]. This shows that the bare AuNPs immobilized onto the nitrided CVD carbon substrate were highly electrocatalytic toward methanol oxidation. For comparison, Liu and coworkers observed peak current densities at 1.11 V vs. RHE for electrocatalytic oxidation of 1 M methanol in 0.1 M NaOH using ligand-free Au nanoclusters (<2 nm) immobilized on a nitrided carbon support. While these results indicate that electrocatalytic particles can be deposited on CVD carbon UMEs using this technique, it is important to note that the deposition process thus far has been difficult to control on this scale, and most AuNPs that were deposited displayed little to no electrocatalytic activity.

CHAPTER 4

CONCLUSIONS

Understanding the structure-function relationship of nanoparticles is necessary to utilize their full benefits in electrocatalytic application. Several studies have been done to establish the relationship between the electrocatalytic properties of nanoparticles and their structure. However, these studies are mostly done with collections of particles, which are often complicated by factors such as particle heterogeneity and nanoparticle loading. While studies of single, isolated nanoparticles on nanoelectrodes have emerged as promising techniques void of such complications, challenges can still arise from immobilization strategy. In these present studies, immobilization of ligand-free (bare) gold nanoparticles on nitrided CVD carbon electrodes was explored as a means of depositing highly electrocatalytically active metal nanoparticles on ultramicroelectrodes without the use of any capping agent or polymer layer on the electrode.

Nitrogen groups for immobilization of AuNPs were introduced on CVD carbon electrodes by treatment with ammonium hydroxide. The nitriding procedure appeared to be successful based on the significant catalytic behavior of nitrided CVD carbon electrodes toward hydrogen peroxide reduction. The onset potential for the reduction of H_2O_2 on the nitrided electrode shifted to a more positive potential (-0.095 V vs. Ag/AgCl) compared to that of the unmodified electrode (-0.199 V vs. Ag/AgCl). While several attempts to immobilize gold nanoparticles onto untreated carbon ultramicroelectrodes proved to be unsuccessful, nitriding of the same electrodes resulted in successful immobilization of nanoparticles with significant gold oxide and oxide-reduction peaks occurring mainly at 1.1 to 1.2 V and 0.60 to 0.85 V vs. Ag/AgCl, respectively, when cyclic voltammograms were taken in 0.1 M $HClO_4$.

Attempts to characterize the immobilized gold nanoparticles via electrochemical particle sizing methods (surface area-to-volume ratio and oxidative dissolution peak potential in bromide solution) suggested that the particles deposited were mainly large aggregates with relatively high surface coverage. These large aggregates of particles were obtained probably because of the relatively smaller-sized electrodes with undeniably limited number of nucleation sites used in these studies compared to reports that used carbon black and other high surface area carbon sources[66,63]. While electrochemical particle sizing methods indicated that mostly large aggregates were obtained, some of the bare gold nanoparticles showed remarkable electrocatalytic efficiency toward methanol oxidation in alkaline medium (oxidation peak centered at 0.361 V vs. SCE).

Future studies will seek to optimize the various parameters such as concentration of both gold and sodium borohydride solution, deposition time and pH and to carry out electrocatalytic studies of single gold nanoparticle. Since in a couple of occasions, characterization of the particles using potential peak positions contradicted electrochemical SA/V measurements, size determination using imaging techniques could be used to obtain more conclusive results. Due to difficulties in controlling deposition of gold nanoparticles using chemical means, other deposition methods like electrodeposition can also be explored. Future works will also seek to analyze the main types of nitrogen groups using techniques such as X-ray photoelectron spectroscopy. Finally, these methods can be extended to single nanoparticle studies by using relatively smaller-sized chemical vapor deposited electrodes.

REFERENCES

(1) Schuster, R.; Kirchner, V.; Xia, X. H.; Bittner, A. M.; Ertl, G. Nanoscale Electrochemistry. *Phys. Rev. Lett.* **2012**, *80* (25), 5599–5602.

(2) Luo, X.; Morrin, A.; Killard, A. J.; Smyth, M. R. Application of Nanoparticles in Electrochemical Sensors and Biosensors. *Electroanalysis* **2006**, *18* (4), 319–326.

(3) Wang, J. Nanomaterial-Based Electrochemical Biosensors. *Analyst* **2005**, *130* (4), 421–426.

(4) Zamborini, F. P.; Bao, L.; Dasari, R. Nanoparticles in Measurement Science. *Anal. Chem.* **2012**, *84* (2), 541–576.

(5) Sun, P.; Li, F.; Yang, C.; Sun, T.; Kady, I.; Hunt, B.; Zhuang, J. Formation of a Single Gold Nanoparticle on a Nanometer-Sized Electrode and Its Electrochemical Behaviors. *J. Phys. Chem. C* **2013**, *117* (12), 6120–6125.

(6) Mirkin, M. V.; Sun, T.; Yu, Y.; Zhou, M. Electrochemistry at One Nanoparticle. *Acc. Chem. Res.* **2016**, *49* (10), 2328–2335.

(7) Xiao, X.; Pan, S.; Jang, J. S.; Fan, F. R. F.; Bard, A. J. Single Nanoparticle Electrocatalysis: Effect of Monolayers on Particle and Electrode on Electron Transfer. *J. Phys. Chem. C* **2009**, *113* (33), 14978–14982.

(8) Kleijn, S. E. F.; Lai, S. C. S.; Koper, M. T. M.; Unwin, P. R. Electrochemistry of Nanoparticles. *Angew. Chemie - Int. Ed.* **2014**, *53* (14), 3558–3586.

(9) Grunwaldt, J. D.; Kiener, C.; Wögerbauer, C.; Baiker, A. Preparation of Supported Gold Catalysts for Low-Temperature CO Oxidation via "Size-Controlled" Gold Colloids. *J. Catal.* **1999**, *181* (2), 223–232.

(10) Sugunan, A.; Thanachayanont, C.; Dutta, J.; Hilborn, J. G. Heavy-Metal Ion Sensors Using Chitosan-Capped Gold Nanoparticles. *Sci. Technol. Adv. Mater.* **2005**, *6* (3-4 SPEC. ISS.), 335–340.

(11) Wang, L. H.; Huang, W. S. Electrochemical Oxidation of Cysteine at a Film Gold Modified Carbon Fiber Microelectrode Its Application in a Flow-through Voltammetric Sensor. *Sensors* **2012**, *12* (3), 3562–3577.

(12) Pierrat, S.; Zins, I.; Breivogel, A.; S??nnichsen, G. Self-Assembly of Small Gold Colloids with Functionalized Gold Nanorods. *Nano Lett.* **2007**, *7* (2), 259–263.

(13) Jain, P. K.; Huang, X.; El-sayed, I. H.; El-sayed, M. A. Noble Metals on the Nanoscale : Optical and Photothermal Properties and Some Applications. *Am. Chem. Soc. Acc. Chem. Res.* **2008**, *41* (12), 7–9.

(14) Kwon, Y.; Kim, M. G.; Kim, Y.; Lee, Y.; Cho, J. Effect of Capping Agents in Tin

Nanoparticles on Electrochemical Cycling. *Electrochem. Solid-State Lett.* **2006**, *9* (1), A34–A38.

(15) Xiao, X.; Bard, A. J. Observing Single Nanoparticle Collisions at an Ultramicroelectrode by Electrocatalytic Amplification. *J. Am. Chem. Soc.* **2007**, *129* (31), 9610–9612.

(16) Yan, S.; Zhang, S.; Lin, Y.; Liu, G. Electrocatalytic Performance of Gold Nanoparticles Supported on Activated Carbon for Methanol Oxidation in Alkaline Solution. *J. Phys. Chem. C* **2011**, *115* (14), 6986–6993.

(17) Shao, M.; Peles, A.; Shoemaker, K. Electrocatalysis on Platinum Nanoparticles: Particle Size Effect on Oxygen Reduction Reaction Activity. *Nano Lett.* **2011**, *11* (9), 3714–3719.

(18) Afraz, A.; Rafati, A. A.; Hajian, A.; Khoshnood, M. Electrodeposition of Pt Nanoparticles on New Porous Graphitic Carbon Nanostructures Prepared from Biomass for Fuel Cell and Methanol Sensing Applications. *Electrocatalysis* **2015**, *6* (2), 220–228.

(19) Somorjai, G. A.; Contreras, A. M.; Montano, M.; Rioux, R. M. Clusters, Surfaces, and Catalysis. *Proc. Natl. Acad. Sci.* **2006**, *103* (28), 10577–10583.

(20) Bergamaski, K.; Pinheiro, A. L. N.; Teixeira-Neto, E.; Nart, F. C. Nanoparticle Size Effects on Methanol Electrochemical Oxidation on Carbon Supported Platinum Catalysts. *J. Phys. Chem. B* **2006**, *110* (39), 19271–19279.

(21) Gamez, A.; Richard, D.; Gallezot, P.; Gloaguen, F.; Faure, R.; Durand, R. Oxygen Reduction Nanoparticles. *Electroehimica Acta* **1996**, *41* (2), 307–314.

(22) Xu, W.; Kong, J. S.; Chen, P. Probing the Catalytic Activity and Heterogeneity of Au-Nanoparticles at the Single-Molecule Level. *Phys. Chem. Chem. Phys.* **2009**, *11* (15), 2767–2778.

(23) Li, Y.; Cox, J. T.; Zhang, B. Electrochemical Responses and Electrocatalysis at Single Au Nanoparticles. *J. Am. Chem. Soc.* **2010**, *132* (9), 3047–3054.

(24) Yu, Y.; Gao, Y.; Hu, K.; Blanchard, P. Y.; Noël, J. M.; Nareshkumar, T.; Phani, K. L.; Friedman, G.; Gogotsi, Y.; Mirkin, M. V. Electrochemistry and Electrocatalysis at Single Gold Nanoparticles Attached to Carbon Nanoelectrodes. *ChemElectroChem* **2015**, *2* (1), 58–63.

(25) Taylor, S.; Fabbri, E.; Levecque, P.; Schmidt, T. J.; Conrad, O. The Effect of Platinum Loading and Surface Morphology on Oxygen Reduction Activity. *Electrocatalysis* **2016**, *7* (4), 287–296.

(26) Kumar, S.; Zou, S. Electrooxidation of Carbon Monoxide on Gold Nanoparticle Ensemble Electrodes: Effects of Particle Coverage. *J. Phys. Chem. B* **2005**, *109* (33), 15707–15713.

(27) Kumar, S.; Zou, S. Electrooxidation of CO on Uniform Arrays of Au Nanoparticles: Effects of Particle Size and Interparticle Spacing. *Langmuir* **2009**, *25* (1), 574–581.

(28) Higuchi, E.; Uchida, H.; Watanabe, M. Effect of Loading Level in Platinum-Dispersed Carbon Black Electrocatalysts on Oxygen Reduction Activity Evaluated by Rotating Disk Electrode. *J. Electroanal. Chem.* **2005**, *583* (1), 69–76.

(29) Nesselberger, M.; Roefzaad, M.; Fayçal Hamou, R.; Ulrich Biedermann, P.; Schweinberger, F. F.; Kunz, S.; Schloegl, K.; Wiberg, G. K. H.; Ashton, S.; Heiz, U.; et al. The Effect of Particle Proximity on the Oxygen Reduction Rate of Size-Selected Platinum Clusters. *Nat. Mater.* **2013**, *12* (10), 919–924.

(30) Guo, Z.; Percival, S. J.; Zhang, B. Chemically Resolved Transient Collision Events of Single Electrocatalytic Nanoparticles. *J. Am. Chem. Soc.* **2014**, *136* (25), 8879–8882.

(31) Wakerley, D.; Güell, A. G.; Hutton, L. A.; Miller, T. S.; Bard, A. J.; Macpherson, J. V. Boron Doped Diamond Ultramicroelectrodes: A Generic Platform for Sensing Single Nanoparticle Electrocatalytic Collisions. *Chem. Commun.* **2013**, *49* (50), 5657–5659.

(32) Zhou, H.; Park, J. H.; Fan, F. R. F.; Bard, A. J. Observation of Single Metal Nanoparticle Collisions by Open Circuit (Mixed) Potential Changes at an Ultramicroelectrode. *J. Am. Chem. Soc.* **2012**, *134* (32), 13212–13215.

(33) Fan, F. R. F.; Bard, A. J. Observing Single Nanoparticle Collisions by Electrogenerated Chemiluminescence Amplification. *Nano Lett.* **2008**, *8* (6), 1746–1749.

(34) Bard, A. J.; Zhou, H.; Kwon, S. J. Electrochemistry of Single Nanoparticles via Electrocatalytic Amplification. *Isr. J. Chem.* **2010**, *50* (3), 267–276.

(35) Xiao, Y.; Fan, F. R. F.; Zhou, J.; Bard, A. J. Current Transients in Single Nanoparticle Collision Events. *J. Am. Chem. Soc.* **2008**, *130* (49), 16669–16677.

(36) Wehmeyer, K. R.; Deakin, M. R.; Wightman, R. M. Electroanalytical Properties of Band Electrodes of Submicrometer Width. *Anal. Chem.* **1985**, *57* (9), 1913–1916.

(37) Zoski, C. G.; Liu, B.; Bard, A. J. Scanning Electrochemical Microscopy: Theory and Characterization of Electrodes of Finite Conical Geometry. *Anal. Chem.* **2004**, *76* (13), 3646–3654.

(38) Robinson, D. A.; Kondajji, A. M.; Castañeda, A. D.; Dasari, R.; Crooks, R. M.; Stevenson, K. J. Addressing Colloidal Stability for Unambiguous Electroanalysis of Single Nanoparticle Impacts. *J. Phys. Chem. Lett.* **2016**, *7* (13), 2512–2517.

(39) Chen, S.; Kucernak, A. Electrodeposition of Platinum on Nanometer-Sized Carbon Electrodes. *J. Phys. Chem. B* **2003**, *107* (33), 8392–8402.

(40) Arrigan, D. W. M. Nanoelectrodes, Nanoelectrode Arrays and Their Applications. *Analyst* **2004**, *129* (12), 1157–1165.

(41) Matthews, J. N. A. Nanoscale Electrochemistry. *Anal. Chem.* **2013**, *85* (10), 473–486.

(42) Cox, J. T.; Zhang, B. Nanoelectrodes: Recent Advances and New Directions. *Annu. Rev. Anal. Chem.* **2012**, *5* (1), 253–272.

(43) Dayton, M. A.; Ewing, A. G.; Wightman, R. M. Response of Microvoltammetric Electrodes to Homogeneous Catalytic and Slow Heterogeneous Charge-Transfer Reactions. *Anal. Chem.* **1980**, *52* (14), 2392–2396.

(44) Dayton, M. A.; Brown, J. C.; Stutts, K. J.; Wightman, R. M. Faradaic Electrochemistry at Microvoltammetric Electrodes. *Anal. Chem.* **1980**, *52* (6), 946–950.

(45) Bond, A. M.; Fleischmann, M.; Robinson, J. Electrochemistry in Organic Solvents without Supporting Electrolyte Using Platinum Microelectrodes. *J. Electroanal. Chem.* **1984**, *168* (1–2), 299–312.

(46) Kittlesen, G. P.; White, H. S.; Wrighton, M. S. Chemical Derivatization of Microelectrode Arrays by Oxidation of Pyrrole and N-Methylpyrrole: Fabrication of Molecule-Based Electronic Devices. *J. Am. Chem. Soc.* **1984**, *106* (24), 7389–7396.

(47) Penner, R. M.; Heben, M. J.; Longin, T. L.; Lewis, N. S. Fabrication and Use of Nanometer-Sized Electrodes in Electrochemistry. *Science (80-.).* **2006**, *250* (4984), 1118–1121.

(48) Sun, P.; Zhang, Z.; Guo, J.; Shao, Y. Fabrication of Nanometer-Sized Electrodes and Tips for Scanning Electrochemical Microscopy. *Anal. Chem.* **2001**, *73* (21), 5346–5351.

(49) Mirkin, M. V; Fan, F.-R. F.; Bard, A. J. Scanning Electrochemical Microscopy Part 13. Evaluation of the Tip Shapes of Nanometer Size Microelectrodes. *J. Electroanal. Chem.* **1992**, *328* (1–2), 47–62.

(50) Katemann, B. B.; Schuhmann, W. Fabrication and Characterization of Needle-Type Pt-Disk Nanoelectrodes. *Electroanalysis* **2002**, *14* (1), 22–28.

(51) Mirkin, M. V. Nanoelectrodes and Liquid/ Liquid Nanointerfaces. In *Nanoelectrochemistry*; Mirkin, M. V, Amemiya, S., Eds.; CRC Press: Boca Raton, FL, 2015; pp 539–572.

(52) Yu, Y.; Noël, J. M.; Mirkin, M. V.; Gao, Y.; Mashtalir, O.; Friedman, G.; Gogotsi, Y. Carbon Pipette-Based Electrochemical Nanosampler. *Anal. Chem.* **2014**, *86* (7), 3365–3372.

(53) Actis, P.; Tokar, S.; Clausmeyer, J.; Babakinejad, B.; Mikhaleva, S.; Cornut, R.; Takahashi, Y.; López Córdoba, A.; Novak, P.; Shevchuck, A. I.; et al. Electrochemical Nanoprobes for Single-Cell Analysis. *ACS Nano* **2014**, *8* (1), 875–884.

(54) Chen, S.; Kucernak, A. Electrocatalysis under Conditions of High Mass Transport Rate: Oxygen Reduction on Single Submicrometer-Sized Pt Particles Supported on Carbon. *J. Phys. Chem. B* **2004**, *108* (10), 3262–3276.

(55) Clausmeyer, J.; Masa, J.; Ventosa, E.; Öhl, D.; Schuhmann, W. Nanoelectrodes Reveal the Electrochemistry of Single Nickelhydroxide Nanoparticles. *Chem. Commun.* **2016**, *52* (11), 2408–2411.

(56) Liu, B.; Yao, H.; Song, W.; Jin, L.; Mosa, I. M.; Rusling, J. F.; Suib, S. L.; He, J. Ligand-Free Noble Metal Nanocluster Catalysts on Carbon Supports via "Soft" Nitriding. *J. Am. Chem. Soc.* **2016**, *138* (14), 4718–4721.

(57) Shi, L.; Niu, X.; Liu, T.; Zhao, H.; Lan, M. Electrocatalytic Sensing of Hydrogen Peroxide Using a Screen Printed Carbon Electrode Modified with Nitrogen-Doped Graphene Nanoribbons. *Microchim. Acta* **2015**, *182* (15–16), 2485–2493.

(58) Gastrectomy, V. S.; Risk, A. Electrocatalytic Oxidation of Alcohols, Tripropylamine, and DNA with Ligand-Free Gold Nanoclusters on Nitrided Carbon. *ChemElectroChem* **2016**, *23* (5), 1079–1084.

(59) Bishop, G. W.; Ahiadu, B. K.; Smith, J. L.; Patterson, J. D. Use of Redox Probes for Characterization of Layer-by-Layer Gold Nanoparticle-Modified Screen-Printed Carbon Electrodes. *J. Electrochem. Soc.* **2016**, *164* (2), B23–B28.

(60) Adams, K. L.; Jena, B. K.; Percival, S. J.; Zhang, B. Highly Sensitive Detection of Exocytotic Dopamine Release Using a Gold-Nanoparticle-Network Microelectrode. *Anal. Chem.* **2011**, *83* (3), 920–927.

(61) Batista, C. A. S.; Larson, R. G.; Kotov, N. A. Nonadditivity of Nanoparticle Interactions. *Science (80-.).* **2015**, *350* (6257), 1242477–10.

(62) Kadara, R. O.; Jenkinson, N.; Banks, C. E. Characterisation of Commercially Available Electrochemical Sensing Platforms. *Sensors Actuators, B Chem.* **2009**, *138* (2), 556–562.

(63) Ben Liu, Huiqin Yao, Wenqiao Song, Lei Jin, Islam M. Mosa, James F. Rusling, Steven L. Suib, and J. H. Ligand-Free Noble Metal Nanocluster Catalysts on Carbon Supports via "Soft" Nitriding. *J. Am. Chem. Soc.* **2016**, *138* (14), 4718–4721.

(64) Affadu-danful, G. Immobilization of Gold Nanoparticles on Nitrided Carbon Fiber Ultramicroelectrodes by Direct Reduction, East Tennessee State University, 2018.

(65) Alexeyeva, N.; Tammeveski, K. Electroreduction of Oxygen on Gold Nanoparticle/PDDA-MWCNT Nanocomposites in Acid Solution. *Anal. Chim. Acta* **2008**, *618* (2), 140–146.

(66) Sharma, J. N.; Pattadar, D. K.; Mainali, B. P.; Zamborini, F. P. Size Determination of Metal Nanoparticles Based on Electrochemically Measured Surface-Area-to-Volume Ratios. *Anal. Chem.* **2018**, *90* (15), 9308–9314.

(67) Ivanova, O. S.; Zamborini, F. P. Electrochemical Size Discrimination of Gold Nanoparticles Attached to Glass/Indium-Tin-Oxide Electrodes by Oxidation in Bromide-Containing Electrolyte. *Anal. Chem.* **2010**, *82* (13), 5844–5850.

(68) Plieth, W. J. Electrochemical Properties of Small Metal Clusters. *J. Phys. Chem.* **1982**, *86* (16), 3166–3170.

(69) Henglein, A. Physicochemical Properties of Small Metal Particles in Solution: "Microelectrode" Reactions, Chemisorption, Composite Metal Particles, and the Atom-to-Metal Transition. *J. Phys. Chem.* **1993**, *97* (21), 5457–5471.

VITA

ENOCH AMOAH

Education:	MSc Chemistry, East Tennessee State University, Johnson City, Tennessee, 2019.
	B.Sc. Chemistry, Kwame Nkrumah University of Science and Technology, Kumasi, Ghana, 2016.
Professional Experience:	Graduate Teaching Assistant, East Tennessee State University, Johnson City, TN, 2017-2019.
	Research Assistant, (Dr. Gregory Bishop's Research Lab), East Tennessee State University, Johnson City, TN, 2019.
	Teaching Assistant, Kwame Nkrumah University of Science and, Technology, Kumasi, Ghana, 2016 – 2017.
Research Experience:	Graduate research student, East Tennessee State University, Johnson City, TN, 2017-2019 (Mentor: Dr. Gregory W. Bishop).
	Undergraduate research student, Kwame Nkrumah University of Science and Technology, Kumasi, Ghana, 2015-2016 (Mentor: Dr. Mercy Badu).
Presentations:	Enoch Amoah, Daniel Mawudoku, Gregory W. Bishop. Modification of Chemical Vapor-Deposited Carbon Electrodes with Electrocatalytic Metal Nanoparticles through a Soft Nitriding Technique, 70th South East Regional Meeting of the American Chemical Society, 11/01/2018, Augusta, GA, Poster Presentation.
	Daniel Mawudoku, Enoch Amoah, Gregory W. Bishop. Nitrogen-doping of Carbon Fiber Electrodes as a Strategy for Immobilization and Characterization of Electrocatalytically Active Gold Nanoparticles, 2018 Eastman-NETSACS Student Research Symposium, 10/16/2018, Kingsport, TN, Poster Presentation.
	Enoch Amoah, Daniel Mawudoku, Gregory W. Bishop. Modification of Chemical Vapor-Deposited Carbon Electrodes with Electrocatalytic Metal Nanoparticles through a Soft Nitriding Technique, Graduate Seminar, Chemistry Department, East

Tennessee State University, Johnson City, TN, 02/22/2019, oral Presentation.

Honors and Awards: The Margaret Sells Endowment Scholarship Award, Outstanding Achievement in the Field of Chemistry in the College of Arts and Sciences, East Tennessee State University, Johnson City, TN, 11/03/2017